Spatial Fading Channel Emulation for Over-the-air Testing of mmWave Radios: Concepts and Experimental Validations

Wei Fan, Lassi Hentilä, and Pekka Kyösti

***Abstract*—Millimeter wave (mmWave) communication is regarded as the key enabling component for 5G cellular systems due to the large amount of available spectrum. To make mmWave new radio (NR) a reality, tremendous efforts have been exerted from the industry and academia. Performance evaluation of mmWave NR is a mandatory step and the key to ensure the success of mmWave 5G deployment. Over-the-air (OTA) radiated testing method for mmWave new radio (NR) in laboratory conditions is highly attractive, since it makes possible to achieve virtual field testing purposes of mmWave devices in realistic propagation conditions. In this paper, we first discuss the need and challenges for OTA measurement of mmWave 5G NR under fading channel conditions. After that, two promising candidate solutions: i.e. wireless cable and multi-probe anechoic chamber (MPAC), are detailed. Their principles, applicability for mmWave NR and main challenges are discussed. Furthermore, preliminary experimental validations results in a frequency range (FR) 2 anechoic chamber are demonstrated for the wireless cable and MPAC methods at 28 GHz.**

***Index Terms*—Spatial channel model, over-the-air (OTA) testing, wireless cable method, multi-probe anechoic chamber (MPAC) method, FR2 validation.**

I. Introduction

Millimeter wave (mmWave) communication is seen as the key enabling technology to achieve high data-rate transmission [1]–[4]. To make mmWave 5G new radio (NR) (i.e. the global 5G standard) a success, tremendous efforts have been exerted from academia, industry, and government laboratories in the past few years. Many 5G field trials and test-bed platforms have been reported by key industrial and academic players [2], where the objective is to demonstrate and validate whether 5G key performance indicators (KPIs) can be met in various representative real-world deployment scenarios. However, field trials are expensive and uncontrollable. If systems fail in field trials, it is difficult and complicated to identify the root cause, due to the lack of controllable and repeatable testing environment.

For sub-6 GHz antenna systems, accessible antenna connectors are typically implemented for cable conducted testing purposes. However, it is predicted that the conducted testing will no longer be applicable for mmWave NRs, due to the lack of antenna connectors [5]–[13]. mmWave antennas will be small, highly integrated units (e.g., antenna on chip or antenna in package), and possibly with a massive antenna count. Therefore, mmWave NR testing will move exclusively to over-the-air (OTA) radiated modes using the device antennas as the direct interface to the test system. This also allows the possibility to take into consideration mmWave antenna systems in the performance testing.

Historically, OTA testing has been used to evaluate radio performance of antenna systems. OTA testing of single-antenna user terminals (UEs) was standardized more than a decade ago [14]. OTA testing for sub-6 GHz LTE multiple-input multiple-output (MIMO) terminals has been standardized in the cellular telecommunications industry association (CTIA) and the 3rd generation partnership project (3GPP) standards, where the multi-probe anechoic chamber (MPAC) and radiated two stage (RTS) methods were selected and standardized [8], [9], [15]. The automotive industry also started to adopt OTA testing solutions for sub-6GHz MIMO systems to ensure reliable wireless communication in dynamic vehicle-to-vehicle (V2V) and vehicle-to-infrastructure (V2X) scenarios [16], [17]. Strong efforts have been taken in 3GPP recently to standardize test methodology for the verification of multi-antenna reception performance of NR user equipment (UE) [18]. For frequency region 1 (FR1), i.e. frequency range 450 MHz – 6000 MHz, two-dimension (2D) MPAC test method is the reference methodology, while RTS test method is selected as the harmonized methodology. For FR2, which corresponds to frequency range 24.25 GHz – 52.6 GHz, the three-dimension (3D) simplified MPAC test sectup is selected as the reference methodology.

One essential step in the research and development stage is to validate 5G radios under ideal and clean RF propagation channel conditions. For example, plane wave condition is adopted as default reference for antenna and radio frequency (RF) transceiver characterization, including antenna radiation pattern, transmitter and receiver radiated performance, antenna array calibration, etc. Several strategies to mimic plane wave testing condition, e.g. direct far-field chamber, compact antenna testing range (CATR), plane wave generator (PWG) and near-field to far field transformation techniques have been reported [19]. It is also of great importance to optimize and validate the device performance in real-world conditions, i.e. under faded and subject to interference channel conditions with multiple cells, users, and radio access technologies. Therefore, channel emulators (CEs), which are typically used

Wei Fan is with the Antenna Propagation and Millimeter-wave Systems (APMS) section, Department of Electronic Systems, Aalborg University, 9220 Aalborg, Denmark.

Lassi Hentilä and Pekka Kyösti are with Keysight Technologies Finland Oy, Oulu, Finland

Pekka Kyösti is also with Centre for Wireless Communications, University of Oulu, 90014 Oulu, Finland

to emulate the radio channel between the transmitter (Tx) and the receiver (Rx), are extensively utilized for end-to-end real-world performance testing for wireless devices and base stations in the lab [20]. It would be desirable to develop cost-effective OTA testing methodologies in laboratory conditions, which makes it possible to achieve virtual field testing purposes of mmWave devices in realistic conditions. This enables testing all mmWave 5G KPIs in various reproduced scenarios (including 5G friendly or 5G hostile scenarios) in a controllable way. By doing so, the engineer has the possibility to quickly verify performance of the mmWave NR and to quickly test how hardware and software design changes affects the NR system performance. The goal is to develop an OTA testing methodology suitable to evaluate mmWave NR in a realistic, reliable, repeatable, and cost-efficient way in laboratory conditions, thereby ensuring timely and efficient development and optimization of mmWave devices. There is a strong need for a standard and cost-effective testing solution from the industry and government laboratories, since mmWave OTA testing is required for the success of mmWave 5G deployment.

In this work, the main focus is on spatial fading channel emulation for OTA testing of mmWave radios and its validation in a practical FR2 anechoic chamber. Validation of spatial fading channel emulation in FR1 has been extensively discussed in the literature [**?**], [15], [21]. However, no work has been reported on validation in the FR2 chamber. There are some practical difference of validation at the FR1 and FR2 chamber. The probe antennas and measurement antennas are more directive at the FR2. Virtual array, which is used to estimate the emulated channel spatial profile in the chamber, will be more difficult to form with the mechanical positioner, as the wavelength at the FR2 is much smaller. The channel emulation at FR2 is also more complicated, which involves frequency up-and-down conversion for the sub-6 GHz channel emulator. To bring mmWave OTA testing from theory to practice, we also must ask to what extent the theoretical analysis can be maintained in realistic testing setups. Most work on mmWave OTA testing in spatial fading channels presented in the literature is limited to theoretical analysis via numerical simulations, clearly lacking experimental validation in practical mmWave OTA setups [7]–[9]. In this paper, we experimentally validated the wireless cable method and MPAC method in a practical setup for mmWave NR testing. We first discuss two OTA methods that are capable of emulating spatial fading channels. Two simple strategies to achieve wireless cable connection for mmWave radios, i.e. employing antenna polarization discrimination and pattern discrimination, are proposed. Their applicability and limitations to mmWave radios are discussed. The main contributions of the paper are:

- The main work is spatial fading channel emulation for OTA testing of mmWave radio and its experimental verification in the actual FR2 anechoic chamber, which has not been reported in the literature yet.
- The method of using antenna pattern diversity and polarization diversity scheme is proposed to achieve wireless cable connection for mmWave radios and it is also experimentally validated.

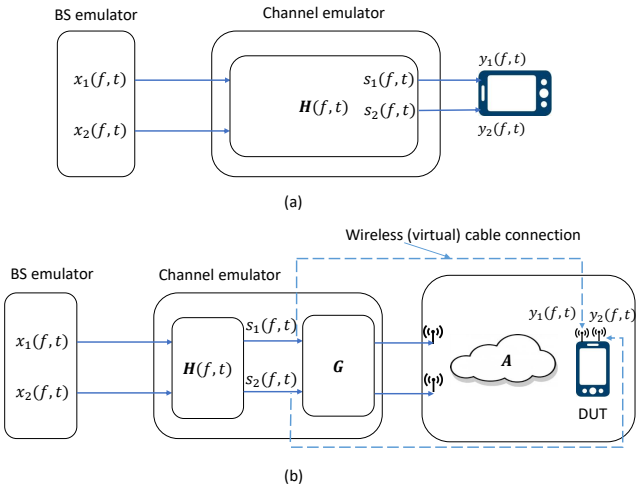

Figure 1. An illustration of the conducted cable setup (a) and the wireless cable setup for mobile handset supporting 2×2 MIMO.

The paper is organized as follows. In Section II, the focus is on wireless cable method. We first discuss the basic idea and how to achieve wireless cable method using different strategies. After that, we demonstrate experimental validation results. The MPAC method is discussed in Section III. We also briefly revisit its basic principle, and how it is adopted in the standardization for 4G and 5G UEs. The spatial correlation and power angle spectrum are measured and validated in the FR2 chamber. Section IV concludes the paper.

II. Wireless Cable Method

A. Principle

In the cable conducted testing setup as shown in Fig. 1 (a), the output ports of the CE are directly coupled to the antenna ports of the MIMO device with coaxial radio frequency (RF) cables. That is, RF cables are used to directly guide testing signals to respective antenna ports, bypassing (most likely internal) antennas from the MIMO device. A photo is shown in Fig. 2 for a LTE handset supporting multi-band 4×4 MIMO. As we can see, it is getting more and more problematic for the traditional cable conducted setup, as the number of receive antennas and frequency bands continue to increase for future UEs .

Wireless (virtual) cable method, which aims to achieve coaxial cable functionality (i.e. signals guided to respective antenna ports with high isolation to cross-talk links) over-the-air, has attracted great research attention recently from both industry and academia [**?**], [22]–[24]. As illustrated in Fig. 1 (b), the basic concept is that the measured static transfer function matrix from probe antenna ports to DUT antenna ports can be calibrated out in the CE.

In the cable conducted setup as illustrated in Fig. 1 (a), the signal model can be written as (ignoring the noise at the Rx side and assuming ideal transmission, i.e. balanced power and no cross-talk among RF cables):

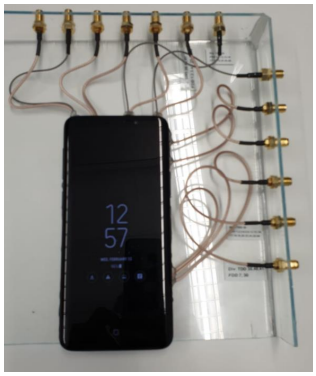

Figure 2. A photo of a commercial LTE mobile handset supporting multi-band 4×4 MIMO.

$$\boldsymbol{y}(f,t) = \boldsymbol{s}(f,t) = \boldsymbol{H}(f,t)\boldsymbol{x}(f,t), \quad (1)$$

where we have the time-variant channel frequency response matrix $\boldsymbol{H}(f,t) \in \mathbb{C}^{N\times M}$ between the M Tx antenna ports and N Rx antenna ports, the received signal vector $\boldsymbol{y}(f,t) \in \mathbb{C}^{N\times 1}$ at the N Rx antenna ports, the transmitted signal vector $\boldsymbol{x}(f,t) \in \mathbb{C}^{M\times 1}$ at the M Tx antenna ports and the testing signal vector to be directed to the N Rx antenna ports $\boldsymbol{s}(f,t) \in \mathbb{C}^{N\times 1}$.

In the wireless cable setup as as illustrated in Fig. 1 (b), the signal model can be written as:

$$\boldsymbol{y}(f,t) = \boldsymbol{A}\boldsymbol{G}\boldsymbol{s}(f,t) = \boldsymbol{A}\boldsymbol{G}\boldsymbol{H}(f,t)\boldsymbol{x}(f,t) = \boldsymbol{H}(f,t)\boldsymbol{x}(f,t), \quad (2)$$

where $\boldsymbol{A} \in \mathbb{C}^{N\times K}$ is the transfer function matrix between the K probe antenna ports and N Rx antenna ports to be measured. $\boldsymbol{G} \in \mathbb{C}^{K\times N}$ is the compensation matrix to approximate $\boldsymbol{A}\boldsymbol{G} = \boldsymbol{I}_{N\times N}$. The actual channel model that is implemented in the CE is $\boldsymbol{H}_{ce}(f,t) = \boldsymbol{G}\boldsymbol{H}(f,t)$. The main challenge of the wireless cable method is how to efficiently obtain the static transfer function matrix in the calibration stage for commercial MIMO devices.

From (2), it is clear that $K \geq N$ should be met to ensure that the target $\boldsymbol{A}\boldsymbol{G} = \boldsymbol{I}_{N\times N}$ can be approximated. For receiver with digital structure, i.e. one RF chain per antenna radiating element, the number of probe antennas (thereby corresponding CE RF interface ports) should be no less than the number of DUT antennas. For receiver with analog or hybrid structure, i.e. one RF chain corresponding to a set of radiating elements, the number of probe antennas should be no less than the DUT RF chains. Furthermore, the transfer function matrix $\boldsymbol{A}$ should be invertible (well-conditioned), static (i.e. non-adaptive to received signals), and preferably frequency independent. Moreover, DUT antennas are bypassed in the wireless cable setup (as in the conducted testing setup), i.e. DUT antennas not included in the testing by default. However, their antenna patterns, if known, can be indirectly considered in the CE during testing.

B. Application for Sub-6 GHz radios

For sub-6 GHz mobile handsets and automobiles, DUTs are typically equipped a few antennas, with unknown antenna designs and locations. The antenna radiation pattern is often quasi-omnidirectional with unknown polarization. Furthermore, in a compact measurement setup, multiple propagation paths exist between the probe antennas and the DUT antennas. Consequently, the transfer transfer function matrix $\boldsymbol{A}$ is an unknown non-identity matrix. Therefore, it must be measured and calibrated out in the CE to achieve wireless cable connection.

Many strategies have been reported in the literature to obtain $\boldsymbol{A}$, depending on the available output information from the DUT. It was shown in [21], [25] that $\boldsymbol{A}$ can be directly calculated based on the knowledge of complex antenna patterns of the DUT. This method, however, requires a large anechoic chamber for far field antenna pattern measurement and support from a special chip-set to report DUT complex antenna patterns in a non-intrusive manner. In [23], it was demonstrated that $\boldsymbol{A}$ can be directly estimated via channel estimation algorithms, e.g. utilizing pilot sequence. This idea, however, might only be supported by base station (BS) type DUT where transmitted signals can be designed and therefore known. In [**?**], based on the received Reference Signal Received Power (RSRP) value per DUT antenna port, a calibration method is proposed to determine $\boldsymbol{A}$. The method is highly attractive since the testing can be performed in a small RF shielded enclosure. The method was then extended for high-order MIMO DUT in [24], with a closed-form calibration method.

C. Applicability for mmWave NR

For mmWave mobile handsets, the antenna designs are widely different from sub-6 GHz systems. mmWave radios will rely heavily on beamforming capability to improve link signal to noise ratio (SNR) and track dominant propagation paths in the dynamic channel. Therefore, DUT antenna patterns will be directive and adaptive. As discussed, the transfer matrix $\boldsymbol{A}$ should maintain static to establish the wireless cable connection. As a result, antenna patterns on the DUT should be fixed during testing (i.e. so-called beam-locked mode).

It is defined in 3GPP release 15 [26] that for a 2×2 MIMO system spatial multiplexing is realized using the polarization domain, i.e. one data stream per orthogonal polarization. High-order MIMO system will be defined in the future utilizing the multi-antenna domain. The unique features of mmWave antennas open up new possibilities to achieve wireless cable connection. A straightforward way to achieve wireless cable connection is to design the transfer function matrix $\boldsymbol{A}$ such that $|\boldsymbol{A}| = \boldsymbol{I}$ can be directly approximated in the multi-probe setup, saving the need to compensate it in the CE. As illustrated in the Fig. 3 (top), if the DUT can form widely-separated directive beam patterns, each towards a directive and direction-aligned probe antenna, we can achieve cable-like connection over-the-air via antenna pattern discrimination. Alternatively, polarization discrimination is another way to achieve virtual cable connection for 2×2 MIMO systems, as illustrated in Fig. 3 (below). The wireless cable can be directly achieved via adopting orthogonality between two cross-polarized components, where two wireless cable connections can be achieved.

As explained, the basic idea of the wireless cable concept is that we need to determine the transfer function matrix $\boldsymbol{A}$ and

then calibrate it out. In some special cases, we can directly design the transfer function matrix $\boldsymbol{A}$ such that $|\boldsymbol{A}| = \boldsymbol{I}$ can be approximated in the multi-probe setup. Therefore, there is no need to calibrate it out. In the paper, two proposed schemes, i.e. polarization discrimination and antenna pattern discrimination, are two examples to approximate this special condition $|\boldsymbol{A}| = \boldsymbol{I}$. However, to exploit the antenna pattern discrimination scheme, the DUT must be able to form widely separated directive beam patterns, each towards a directive and direction-aligned probe antenna. To exploit the polarization discrimination scheme, the DUT must support two orthogonal polarizations, each aligned with the polarization of one probe antenna. This strategy is not generic for any DUT, and in any multi-probe setup. For small mmWave user terminals (UEs), it might be not practical to design many widely separated beams due to design limitations. As for polarization discrimination case, it is only limited to 2×2 MIMO systems and MIMO handsets with two orthogonal linear polarized antenna designs. Therefore, transfer function matrix $\boldsymbol{A}$ might not approximate an identity matrix in practice in a general sense. The more general calibration method, which can determine the transfer function matrix $\boldsymbol{A}$ without relying on DUT antenna radiation properties and multi-probe setup, is therefore more generic to achieve wireless cable connection. A generic scheme to achieve wireless cable connection for any DUT is proposed in [27] for 2×2 MIMO and in [28] for high-order MIMO devices. The method requires monitoring the average received power per DUT antenna port in the calibration stage and was validated for sub-6 GHz devices. So far it has not been validated for commercial mmWave devices due to lack of experimental facilities and this part will be addressed in future work.

D. Experimental Validation

1) Measurement Setups: The system diagram of the measurement setup for validating the wireless cable method is shown in Fig. 4. A vector network analyzer (VNA) is utilized to record the channel frequency response (CFR) S21 and S41. A sub-6 GHz CE is extended to the mmWave CE using frequency mixers to up-convert and down-convert signal frequency [20]. An analog signal generator is used to generate the local oscillator (LO) frequency. The frequency conversion is marked in red texts in Fig. 4. The analog signal generator, VNA and CE are synchronized using the 10 MHz reference connection.

For validation purpose, time-invariant channel impulse responses (CIRs) are loaded in the CE. $h_{11}(\tau)$ is a single tap channel with path power 0 dB and $\tau = 0$ ns, while $h_{22}(\tau)$ is also a single tap channel with path power 0 dB and $\tau = 935$ ns. $h_{21}(\tau)$ and $h_{12}(\tau)$ are disabled in the CE. The different tap delay values in $h_{11}(\tau)$ and $h_{22}(\tau)$ are intentionally designed to check how well wireless cable connections are achieved. For ideal wireless cable connections, $h_{11}(\tau)$ and $h_{22}(\tau)$ can only be recorded in the first (i.e. S_{21} measurement) and second DUT antenna (i.e. S_{41} measurement), respectively, with no cross-talk to the other DUT antenna. Therefore, we can easily check how well the wireless cable connection is established

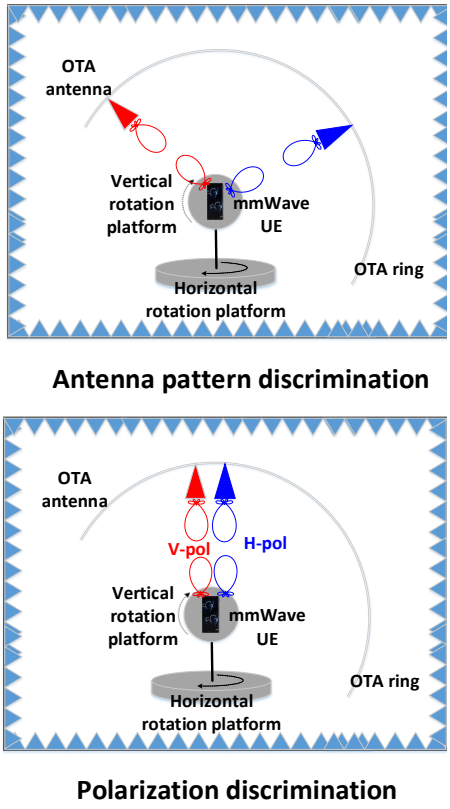

Figure 3. An illustration of achieving wireless cable connection via antenna pattern discrimination (top) and antenna polarization discrimination (below).

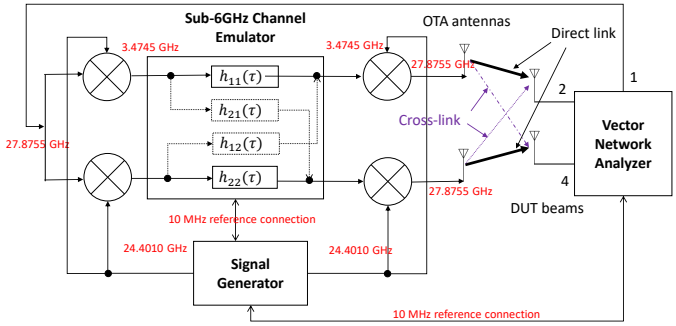

Figure 4. System diagram for the wireless cable method validation setup.

by comparing the power values at the two different delay taps on each DUT receive antenna.

A photo of the measurement setup inside the anechoic chamber for the wireless cable method using polarization discrimination scheme and antenna pattern discrimination scheme is shown in Fig. 5 and Fig. 6, respectively. The measurement was done in a FR2 anechoic chamber in Keysight technologies, Finland. Two dual-polarized probe antennas on a ring (each with two polarization feed antenna ports) were used. Two linearly-polarized standard gain horn antennas operating at 28 GHz were used to mimic two beams formed by the mmWave DUT. According to [29], the reference antenna under test (AUT) for FR2 UE shall be a directive antenna, where the HPBW of reference antenna at 28 GHz in the H-plane ranges from around 15^o to 30^o. The HPBW of the horn antenna in

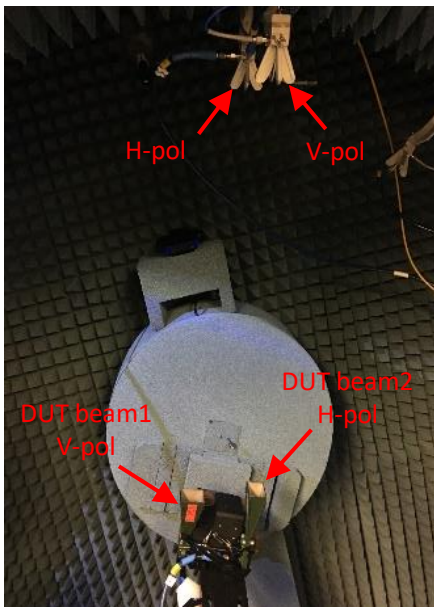

Figure 5. Measurement setup for wireless cable method using polarization discrimination scheme.

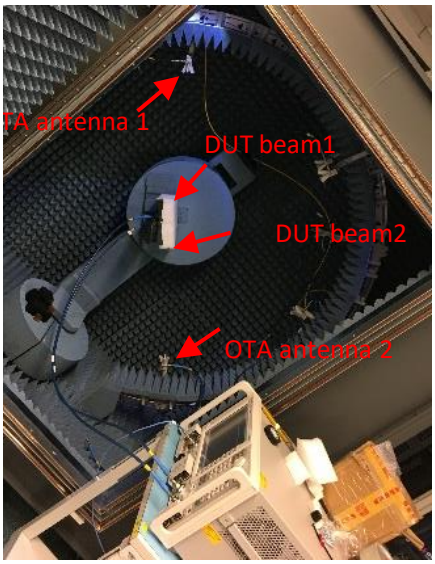

Figure 6. Measurement setup for wireless cable method using antenna pattern discrimination.

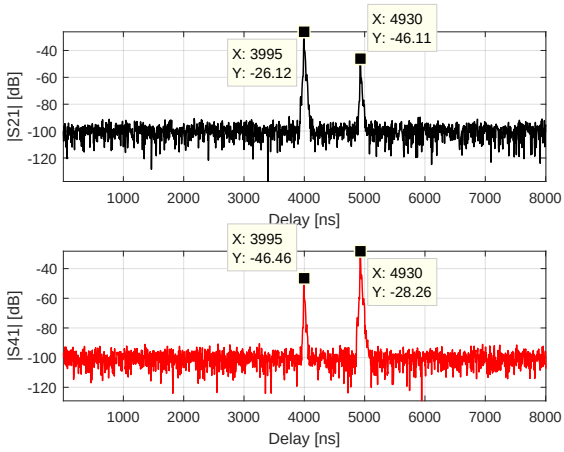

Figure 7. Measured CIRs for the first (S21) and second DUT antenna (S41) using polarization discrimination scheme.

the measurement is around 20^o, which is suitable to mimic FR2 UE beams.

The DUT antennas were placed on a turntable in the center of the chamber, with a distance of around 1 m to the probe antennas on the ring. To enable polarization discrimination scheme, the H-pol port on one probe antenna and the V-pol port on the other probe antenna are connected to the mmWave CE output ports. At the DUT side, one DUT antenna is aligned to the V-pol of the probe antenna, while the other DUT antenna is rotated 90^o to align with the the H-pol of the other probe antenna, as shown in Fig. 5. To mimic wireless cable connection employing antenna pattern discrimination scheme, the probe configuration and DUT antenna configuration are shown in Fig. 6. Basically, the probe antennas are widely separated to minimize cross talks, and two DUT antennas were steered to the respective probe antennas. As seen in Fig. 6, both the probe antennas and measurement antennas are aligned in the vertical polarization, which indicates that only the antenna pattern discrimination is employed in the measurement. In principle, we can further reduce the cross-talk by employing both the antenna pattern and polarization discrimination scheme for 2×2 MIMO.

2) Measurement Results: The measured CIRs at the two DUT antennas can be obtained via performing inverse Fourier transform of the CFRs. The measured CIRs for the first and second DUT antenna using polarization discrimination scheme are shown in Fig. 7. Two taps, with a delay difference of around 935 ns, can be observed from the measured CIR for the first antenna, with the second tap around 20 dB smaller than the first one. This basically indicated that the first wireless cable connection is well established, with around -20 dB cross-talk from the second wireless cable connection. We can make similar observations for the second DUT antenna measurement. Note that there is a path difference of around 2.1 dB for the direct link (i.e. the first tap in S21 and the second tap in S41 measurements). This imbalance should be calibrated out in practice to ensure balanced transmission over wireless cable.

The measured CIRs for the first and second DUT antenna using antenna pattern discrimination scheme are shown in Fig. 8. As we can see, more than 30 dB isolation can be achieved for both wireless cable connections using this simple scheme.

III. MPAC METHOD

A. Principle

The basic idea of the MPAC method is that the signals radiated from the probe antennas are controlled and optimized in the CE such that the reproduced RF environment within the test area will mimic the target spatial fading channel [7], [30]. The main advantage of the MPAC method is that it is a true end-to-end testing solution, which can be used to test off-the-shelf DUTs. Unlike wireless cable method, it works for adaptive DUT without the need to lock antenna beams during

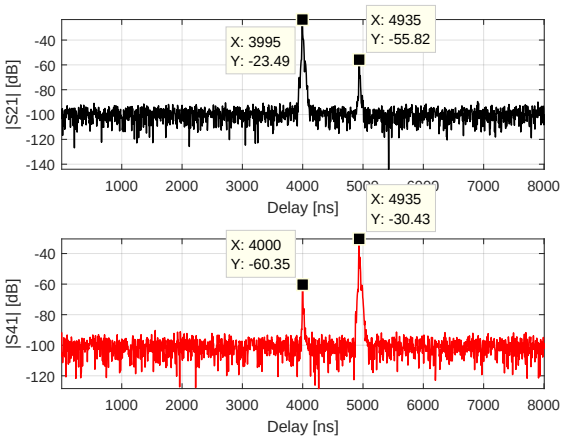

Figure 8. Measured CIRs for the first (S21) and second DUT antenna (S41) using beam pattern discrimination scheme.

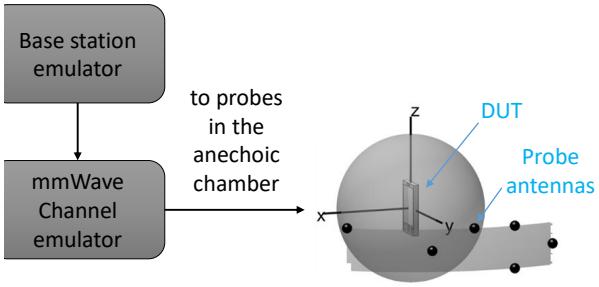

Figure 9. MPAC system layout for FR2 MIMO OTA testing.

testing. The key assumption is that the DUT would operate as it would in the intended propagation environment, but in a repeatable and controllable way. A simple layout for MPAC is shown in Fig. 9.

The signal model can be written as:

$$\boldsymbol{y}(f,t) = \boldsymbol{F}(f,t)\boldsymbol{H}_{CE}(f,t)\boldsymbol{x}(f,t) = \hat{\boldsymbol{H}}(f,t)\boldsymbol{x}(f,t), \quad (3)$$

where $\boldsymbol{H}_{CE}(f,t)$ is the channel model implemented in the CE, and $\boldsymbol{F}(f,t)$ the transfer matrix between the OTA probe antenna port and the DUT antenna port. Time invariant and frequency flat $\boldsymbol{F}$ is often used in the literature, thanks to the non-adaptive DUT and the small fractional bandwidths over carrier frequency. The objective of channel emulation in the MPAC setup is to design $\boldsymbol{H}_{CE}(f,t)$ in the CE such that $\hat{\boldsymbol{H}}(f,t)$ and $\boldsymbol{H}(f,t)$ are statistically similar [31]. The main challenge lies in reproduce the spatial profile of the fading channels, due to discrete OTA probe antenna configurations and limited number of probe antennas, while the other channel parameters (e.g. fading, Doppler profile, delay characteristics, etc.) can be easily reconstructed with a help of a CE. The number of required probe antennas is determined by the spatial discrimination capability of the DUT. Generally speaking, DUT with a large electric size would offer more directive antenna patterns, which in turn would result in the need for dense sampling, i.e. more probe antennas.

B. Applicability for mmWave NR

The MPAC method has been standardized for 4G mobile handset testing in the 2×2 downlink MIMO and transmit diversity mode [15]. For the MPAC configuration, eight dual-polarized probe antennas (which are connected to 16 CE RF interface ports) are placed on a two dimensional (2D) OTA ring. This is mainly due to the fact that 2D spatial channel models (i.e. spatial channel model extended (SCME) urban macro (UMa) and SCME urban micro UMi) are assumed sufficient for performance testing. A uniform probe configuration also has the benefit of offering flexibility to emulate arbitrary spatial channel profiles. The supported test zone size is around 0.8λ.

For MIMO OTA testing of 5G radios, the MPAC setup configurations are different in FR1 and FR2. In FR1, 16 uniformly distributed dual-polarized probe antennas are employed on a 2D OTA ring. This can be seen as a direct extension from the 4G MPAC setup. The channel models are simplified 2D versions of the 3GPP 38.901 channel models (i.e. ignoring the elevation dimension) [18]. The required number of probe antennas is doubled to support a large test zone (in terms of electrical size), thanks to the high operating frequency in FR1 (e.g. up to 5 GHz) compared to 4G LTE bands.

However, for 5G handsets operating at FR2, a different MPAC configuration is adopted due to several reasons [18]. 3D spatial channel modeling is seen as essential to enable 3D beam steering for mmWave antenna systems. Furthermore, the test zone size (in terms of electrical size) is significantly large for mmWave systems, which would necessitate a massive number of OTA antennas and associated CE resources. Therefore, The main challenge for MPAC design in mmWave bands is to reduce system cost yet still ensure realistic fading channels for performance testing. A simple 3D sectored MPAC setup, which consists of six dual-polarized probe antennas, is adopted in the standardization [18], as shown in Fig. [18]. The simple 3D MPAC setup, though limited in flexibility of emulating arbitrary channel models, is proven to be capable of two representative 3D channel models over a large test area [18].

C. Measurement Setup

The system diagram of the measurement setup for validating the MPAC solution is shown in Fig. 10. The VNA transmits signals through the CE and probe antennas. The three probes radiate the faded signals within the anechoic chamber and a receiving test antenna is placed within the test zone. The test antenna is attached to a positioner on the turntable that can move the antenna to pre-defined spatial locations. The received signals are then recorded with the VNA. The vertically polarized antenna feeds of the three probe antennas were connected to the mmWave CE. Three narrowband time-variant channel models were loaded in the CE, with average power 0 dB, -3 dB and -10 dB, respectively. The loaded channel profiles $h_1(t)$, $h_2(t)$ and $h_3(t)$ follow independent and identical distribution (i.i.d.) (complex normal distributions). 10000 channel snapshots were realized for each faded channel profile, with 4 samples per wavelength sampling density [18].

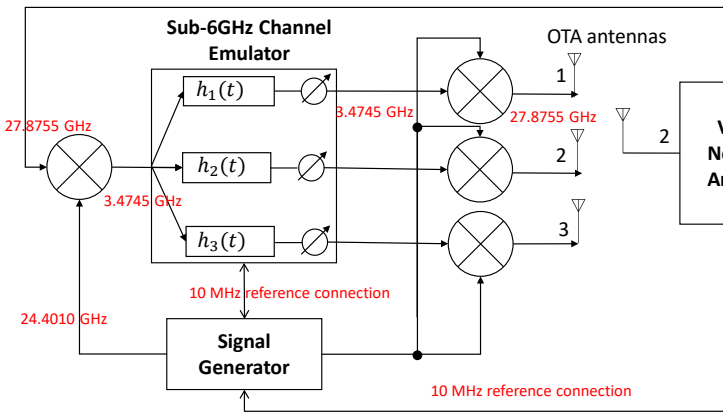

Figure 10. System diagram for the SS-MPAC setup.

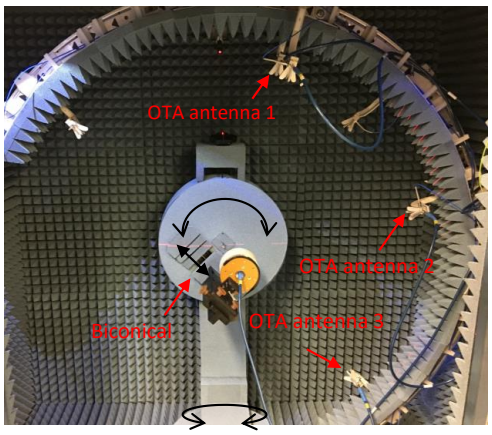

Figure 11. System diagram for the MPAC setup.

A photo of the practical measurement system is shown in Fig. 11. Three dual-polarized probe antennas are on the same ring with an angle separation of 60 degrees. A vertically polarized Biconical antenna [32] with omni-directional antenna pattern in the azimuth plane (i.e. OTA ring) is selected as the test antenna. A virtual linear array in the OTA ring plane is formed by a mechanical linear slide. Virtual array concept is adopted to measure the spatial profile of the emulated channel inside the chamber. Basically, the Biconical antenna is moved to 16 predefined locations (i.e. [0, 0.2, 0.4, 0.6, 0.8, 1, 1.4, 1.8, 2.2, 2.6, 3, 3.4, 3.8, 4.2, 4.6, 5]λ at f_c= 27.876 GHz). Note that the measured locations are smaller than 0.5λ to avoid spatial aliasing problem in the power angle spectrum estimation. The measurement step is as small as 0.2 λ (corresponding to around 2 mm), which demands a highly accurate positioning system. For channel validation in sub-6GHz MIMO OTA testing, a spacing of 0.1 λ was selected (i.e. 1 cm at 3 GHz). In our experimental validation, a spacing of 0.2 λ and 0.4 λ were selected. Note that the physical spacing in the mmWave case is required to be much smaller, i.e. around 2 mm in our measurement compared to 1 cm at 3GHz. Note that as long as the spatial sampling spacing is smaller than 0.5 λ, we can fully capture the spatial characteristics of the channel in the test zone. For each position of the test antenna, we can step and pause the CE to different channel snapshots. Then the CFRs are measured for all stepped channel snapshots. The number of channel snapshots is set to 1000 (i.e. every 10 channel snapshots to ensure independent channel snapshots) and the number of frequency samples is set to 1 (i.e. zero span frequency setting in the VNA). We can then repeat the steps to record CFRs for all 16 spatial sample points.

D. Measurement Results

1) Spatial correlation: The received signals at the virtual array elements (i.e. spatial locations) can be written in a matrix form as:

$$\boldsymbol{r}[t] = \boldsymbol{F}\boldsymbol{s}[t] + \boldsymbol{v}[t] \tag{4}$$

where

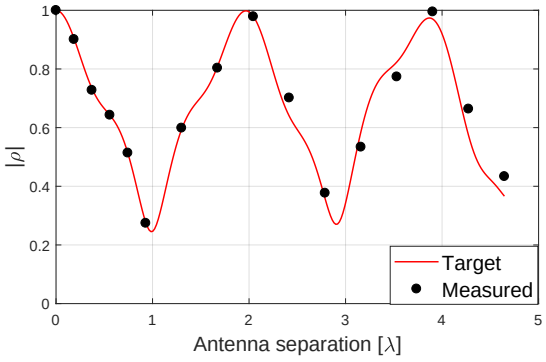

Figure 12. Measured and target spatial correlation in the MPAC setup.

- $\boldsymbol{r}[t] \in \mathbb{C}^{N\times 1}$ is a vector containing N received signals at the t-th snapshot for $t \in [1, T]$,with $T = 1000$.
- $\boldsymbol{F} \in \mathbb{C}^{N\times K}$ is a transfer function matrix of coefficients from the kth probe to the nth test antenna, which can be simplified by the free-space propagation formula.
- $\boldsymbol{s}[t] \in \mathbb{C}^{K\times 1}$ a vector containing K transmitted signals at the t-th snapshot, which is known beforehand.
- $\boldsymbol{v}[t] \in \mathbb{C}^{N\times 1}$ is noise vector, which can be ignored in the validation measurement in the anechoic chamber due to good signal dynamic range.

The autocovariance $\hat{\boldsymbol{R}} \in \mathbb{C}^{N\times N}$ of the received signals can be calculated as:

$$\hat{\boldsymbol{R}} = \frac{1}{T}\sum_{t} \boldsymbol{r}[t]\boldsymbol{r}^H[t] \tag{5}$$

The spatial correlation coefficients among the virtual array elements are the entries from the normalized autocovariance matrix. The measured spatial correlation is shown in Fig. 12. As we can see, the measured spatial correlation matches well with the target curve. The small deviation might be introduced by the limited number of time snapshots, the position accuracy of the practical system, the probe configuration accuracy, etc.

2) Power angle spectra (PAS): The PAS estimate can be obtained

$$\hat{P}(\phi) = \boldsymbol{a}^H(\phi)\hat{\boldsymbol{R}}\boldsymbol{a}(\phi), \tag{6}$$

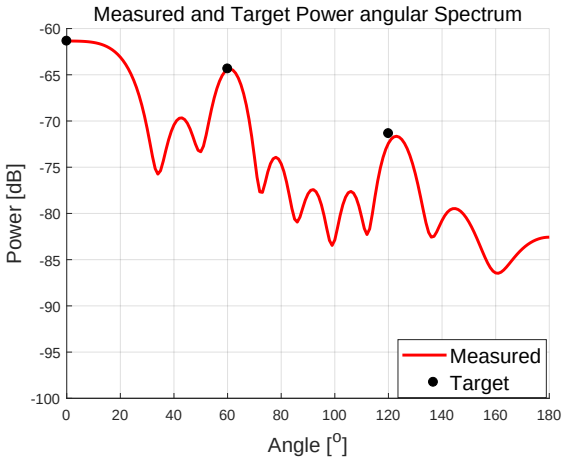

Figure 13. Measured and target power angular spectra in the MPAC setup.

where $\boldsymbol{a}(\phi) \in \mathbb{C}^{N\times 1}$ is the array steering vector of virtual linear array to the angle ϕ. The measured and target PAS in the MPAC setup are shown in Fig. 13. Three peaks can be clearly observed in the measured spectrum. The peak power values, normalized to the first peak, are 0 dB, -3 dB and -10.3 dB, respectively, indicating an excellent agreement with the target values. The peak angles are 0^o, 61^o and 123^o respectively, which also agrees well with the target.

IV. Conclusion

mmWave technology is of vital importance to the design, development, and evaluation of 5G communication system. The focus of the paper is on spatial channel emulation in the anechoic chamber for OTA performance testing of mmWave radios. Two OTA methods have been investigated for mmWave radios with preliminary experimental results, namely the wireless cable method and the multi-probe anechoic chamber (MPAC) method. The measurement was carried out at an FR2 chamber, which has not been reported yet in the literature. Three strategies to achieve wireless cable connection have been discussed, i.e. transfer function matrix calibration, polarization discrimination, and antenna pattern discrimination. It was shown in the preliminary measurement results at around 28 GHz that an isolation more than 20 dB and 30 dB can be achieved for the wireless cable method employing the polarization discrimination and antenna pattern discrimination, respectively. That is, a good wireless cable connection could be easily established for 2×2 MIMO FR2 systems. We also pointed out that transfer function matrix calibration is a more generic strategy for wireless cable method that works for all scenarios. Spatial correlation and power angle spectrum were investigated for the simple MPAC setup in the FR2 chamber. An excellent agreement between the measured results and the target is achieved in terms of spatial correlation and power angle spectrum, which validates the MPAC method in the mmWave bands. The work experimentally validated the application of wireless cable method and the MPAC method in the mmWave NR testing, which will be a valuable input to the ongoing 3GPP standardization.

References

[1] T. S. Rappaport, S. Sun, R. Mayzus, H. Zhao, Y. Azar, K. Wang, G. N. Wong, J. K. Schulz, M. Samimi, and F. Gutierrez, "Millimeter wave mobile communications for 5g cellular: It will work!" *IEEE Access*, vol. 1, pp. 335–349, 2013.

[2] M. Shafi, A. F. Molisch, P. J. Smith, T. Haustein, P. Zhu, P. D. Silva, F. Tufvesson, A. Benjebbour, and G. Wunder, "5g: A tutorial overview of standards, trials, challenges, deployment, and practice," *IEEE Journal on Selected Areas in Communications*, vol. 35, no. 6, pp. 1201–1221, June 2017.

[3] K. Guan, B. Peng, D. He, J. M. Eckhardt, S. Rey, B. Ai, Z. Zhong, and T. Kürner, "Measurement, simulation, and characterization of train-to-infrastructure inside-station channel at the terahertz band," *IEEE Transactions on Terahertz Science and Technology*, vol. 9, no. 3, pp. 291–306, 2019.

[4] ——, "Channel characterization for intra-wagon communication at 60 and 300 ghz bands," *IEEE Transactions on Vehicular Technology*, vol. 68, no. 6, pp. 5193–5207, 2019.

[5] Y. Qi, G. Yang, L. Liu, J. Fan, A. Orlandi, H. Kong, W. Yu, and Z. Yang, "5g over-the-air measurement challenges: Overview," *IEEE Transactions on Electromagnetic Compatibility*, vol. 59, no. 6, pp. 1661–1670, Dec 2017.

[6] M. Rumney, "Testing 5g: Time to throw away the cables," *Microw. J.*, vol. 59, no. 11, 2016.

[7] W. Fan, P. Kyösti, M. Rumney, X. Chen, and G. F. Pedersen, "Over-the-air radiated testing of millimeter-wave beam-steerable devices in a cost-effective measurement setup," *IEEE Communications Magazine*, 2018.

[8] W. Wang, R. Wang, H. Gao, and Y. Wu, "Implementation and analysis of 3d channel emulation method in multi-probe anechoic chamber setups," *IEEE Access*, vol. 7, pp. 108 571–108 580, 2019.

[9] Y. Li, L. Xin, X. Liu, and X. Zhang, "Dual anechoic chamber setup for over-the-air radiated testing of 5g devices," *IEEE Transactions on Antennas and Propagation*, vol. 68, no. 3, pp. 2469–2474, 2020.

[10] Z. Qiao, Z. Wang, W. Fan, X. Zhang, S. Gao, and J. Miao, "Low scattering plane wave generator design using a novel non-coplanar structure for near-field over-the-air testing," *IEEE Access*, vol. 8, pp. 211 348–211 357, 2020.

[11] Y. Zhang, Z. Wang, X. Sun, Z. Qiao, W. Fan, and J. Miao, "Design and implementation of a wideband dual-polarized plane wave generator with tapered feeding nonuniform array," *IEEE Antennas and Wireless Propagation Letters*, vol. 19, no. 11, pp. 1988–1992, 2020.

[12] X. Chen, "Throughput modeling and measurement in an isotropic-scattering reverberation chamber," *IEEE Transactions on Antennas and Propagation*, vol. 62, no. 4, pp. 2130–2139, 2014.

[13] X. Chen, P. Kildal, C. Orlenius, and J. Carlsson, "Channel sounding of loaded reverberation chamber for over-the-air testing of wireless devices: Coherence bandwidth versus average mode bandwidth and delay spread," *IEEE Antennas and Wireless Propagation Letters*, vol. 8, pp. 678–681, 2009.

[14] C. Certification, "Test plan for mobile station over the air performance: Method of measurement for radiated rf power and receiver performance," February 2018.

[15] ——, "Ctia test plan for 2 × 2 downlink mimo and transmit diversity over-the-air performance," September 2017.

[16] M. G. Nilsson, P. Hallbjörner, N. Arabäck, B. Bergqvist, T. Abbas, and F. Tufvesson, "Measurement uncertainty, channel simulation, and disturbance characterization of an over-the-air multiprobe setup for cars at 5.9 ghz," *IEEE Transactions on Industrial Electronics*, vol. 62, no. 12, pp. 7859–7869, Dec 2015.

[17] Y. Ji, W. Fan, M. G. Nilsson, L. Hentilä, K. Karlsson, F. Tufvesson, and G. F. Pedersen, "Virtual drive testing over-the-air for vehicular communications," *IEEE Transactions on Vehicular Technology*, vol. 69, no. 2, pp. 1203–1213, 2020.

[18] 3GPP, "Study on radiated metrics and test methodology for the verification of multi-antenna reception performance of nr user equipment (ue);," June 2020.

[19] K. Technologies, "Ota test for millimeter-wave 5g nr devices and systems," 2018.

[20] W. Fan, P. Kyösti, L. Hentilä, and G. F. Pedersen, "A flexible millimeter-wave radio channel emulator design with experimental validations," *IEEE Transactions on Antennas and Propagation*, vol. 66, no. 11, pp. 6446–6451, 2018.

[21] W. Yu, Y. Qi, K. Liu, Y. Xu, and J. Fan, "Radiated two-stage method for lte mimo user equipment performance evaluation," *IEEE Transactions on Electromagnetic Compatibility*, vol. 56, no. 6, pp. 1691–1696, 2014.

[22] Y. Jing, H. Kong, and M. Rumney, "Mimo ota test for a mobile station performance evaluation," *IEEE Instrumentation Measurement Magazine*, vol. 19, no. 3, pp. 43–50, June 2016.
[23] C. Schirmer, M. Lorenz, W. A. T. Kotterman, R. Perthold, M. H. Landmann, and G. Del Galdo, "Mimo over-the-air testing for electrically large objects in non-anechoic environments," in *2016 10th European Conference on Antennas and Propagation (EuCAP)*, 2016, pp. 1–6.
[24] F. Zhang, W. Fan, and Z. Wang, "Achieving wireless cable testing of high-order mimo devices with a novel closed-form calibration method," *I E E E Transactions on Antennas and Propagation*, Jun. 2020.
[25] M. Rumney, Hongwei Kong, Ya Jing, Zheng Zhang, and P. Shen, "Recent advances in the radiated two-stage mimo ota test method and its value for antenna design optimization," in *2016 10th European Conference on Antennas and Propagation (EuCAP)*, 2016, pp. 1–5.
[26] S. D. Muruganathan, X. Lin, H.-L. Maattanen, J. Sedin, Z. Zou, W. A. Hapsari, and S. Yasukawa, "An overview of 3gpp release-15 study on enhanced lte support for connected drones," *arXiv preprint arXiv:1805.00826*, 2018.
[27] W. Fan, P. Kyösti, L. Hentilä, and G. F. Pedersen, "Mimo terminal performance evaluation with a novel wireless cable method," *IEEE Transactions on Antennas and Propagation*, vol. 65, no. 9, pp. 4803–4814, 2017.
[28] F. Zhang, W. Fan, and Z. Wang, "Achieving wireless cable testing of high-order mimo devices with a novel closed-form calibration method," *IEEE Transactions on Antennas and Propagation*, vol. 69, no. 1, pp. 478–487, 2021.
[29] 3GPP, "Study on test methods," December 2019.
[30] M. D. Foegelle, "The future of mimo over-the-air testing," *IEEE Communications Magazine*, vol. 52, no. 9, pp. 134–142, September 2014.
[31] P. Kyösti, L. Hentilä, W. Fan, J. Lehtomäki, and M. Latva-Aho, "On radiated performance evaluation of massive mimo devices in multiprobe anechoic chamber ota setups," *IEEE Transactions on Antennas and Propagation*, vol. 66, no. 10, pp. 5485–5497, 2018.
[32] W. Fan, I. Carton, J. Ø. Nielsen, K. Olesen, and G. F. Pedersen, "Measured wideband characteristics of indoor channels at centimetric and millimetric bands," *EURASIP Journal on Wireless Communications and Networking*, vol. 2016, no. 1, p. 58, 2016.